

PROCEEDINGS OF SPIE

[SPIDigitalLibrary.org/conference-proceedings-of-spie](https://spiedigitallibrary.org/conference-proceedings-of-spie)

Nanoporous silver films produced by solid-state dewetting for SERS applications

Rusciano, Giulia, Capaccio, Angela, Martinez, Anna, Sasso, Antonio

Giulia Rusciano, Angela Capaccio, Anna Martinez, Antonio Sasso, "Nanoporous silver films produced by solid-state dewetting for SERS applications," Proc. SPIE 11772, Optical Sensors 2021, 117720E (18 April 2021); doi: 10.1117/12.2592391

SPIE.

Event: SPIE Optics + Optoelectronics, 2021, Online Only

Nanoporous silver films produced by solid-state dewetting for SERS applications

Giulia Rusciano^{*1,2}, Angela Capaccio¹, Anna Martinez¹, Antonio Sasso^{1,2}

¹University of Naples "Federico II", Department of Physics "E. Pancini", Via Cintia, I-80126 Naples, Italy

²National Institute of Optics (INO)-National Research Council (CNR), Via Campi Flegrei 34, I-80078, Pozzuoli (NA), Italy

*giulia.rusciano@unina.it

ABSTRACT

Detection of analytes in aqueous solution with high specificity and sensitivity is of paramount importance in many fields of science, ranging from biomedicine, environmental control, and food quality assessment. Surface-enhanced Raman scattering (SERS) has proven to be a cutting-edge analytical technique for this purpose, by combining the high selectivity of Raman features with the high sensitivity deriving from the plasmonic amplification of Raman signals. Herein, we report a facile and quite effective approach to fabricate large-area Ag-based SERS substrates, exhibiting a porous, coral-like nanotexture. Due to their intrinsic large surface-area and high hot-spot density, the produced substrates appear quite promising for the detection of analytes at trace levels. The nanoporous substrates are produced by Solid-State Dewetting (SSD) of thin Ag-films. In particular, ~30 nm thickness Ag-films are first deposited on glass coverslips by magnetron sputtering. Then, marked roughening is induced by exposing the films to an Inductively Coupled Plasma (ICP) discharge, using synthetic air as feeding gas. The performances of our SERS substrates are characterized in terms of morphology and enhancement factor using CV as probe molecule.

Keywords: Raman; SERS; nanoporous Ag film; solid-state dewetting.

1. INTRODUCTION

Nanostructured noble metals, such as Ag and Au, exhibit extraordinary electronic and optical properties, which are mainly related to the possibility of exciting surface plasmon polaritons (SPPs) at the interface between a metal and a dielectric material. SPPs produce huge amplification of the near field which, for nanostructured substrates, can be spatially localized in nanosized regions usually referred as "hotspots" [1]. Recently, silver-based nanoparticles (NPs), such as nanospheres, nano-rods, nano-stars, nano-flowers, nanocubes etc., have attracted most attention since they exhibit tunable resonances covering the entire vis-NIR range [2]. This has pushed forward the application of plasmonic over different fields, among which sensing based on Raman techniques have surely received the main benefit. Raman analysis provides detailed information of the molecular moieties in the samples, enabling their label-free identification [3,4]. Surface-Enhanced Raman Spectroscopy (SERS) preserves this feature, offering a spectacular sensitivity arising from the huge amplification of the Raman signal from analyte molecules in proximity of plasmonic nanostructures. Such amplification is usually expressed in terms of Enhancement Factor (EF), which quantifies the increase of the SERS signal with respect to the spontaneous Raman case. Usually, EF varies in the 10^3 - 10^8 range, although it can reach 10^{14} [5]. Thanks to this feature, SERS has become a reliable and ultrasensitive analytical technique with an increasing number of applications in different fields, ranging from biology, medicine, and environmental monitoring. In particular, SERS-based sensing of biomolecules in aqueous environment has revealed sensitivity up to the single molecule detection [6-8], especially when the probe radiation is resonant with some molecular transition (Surface-Enhanced Resonant Raman Scattering, SERRS). Actually, most of the SERS substrate composed by ordinate arrays of selected NPs exhibit a relatively narrow plasmonic bandwidth, so that it can be used for only one laser line [2]. Moreover, according to SERS mechanism, this prevents the amplification of Raman bands far from the excitation probe wavelength. On the other hand, more complex structures, such as disordered aggregates of colloidal NPs, although exhibiting a much wider plasmonic response, pay the price of a lower

EF spatial reproducibility. In this frame, it is urgent to develop easy, robust and possibly cheap fabrication strategies to produce highly enhancing SERS substrates, exhibiting a broad spectral tunability.

In this paper, we present a rather easy approach to produce nanoporous, silver-based SERS substrates. It is based on the combined use of magnetron sputtering system and an inductively coupled plasma (ICP) system. This method is able to significantly modify the smooth surface of the Ag film prepared by the magnetron making it particularly porous. Intriguingly, thanks to the intrinsic large surface-area of the obtained film and the high hot-spot density, the obtained substrates appear quite promising for the detection of analytes at trace levels. Herein, we report their characterization in terms of morphology and plasmonic performances.

2. MATERIALS AND METHODS

2.1 Raman set-up

The spectroscopic analysis was performed by using a commercial micro-Raman system (WiTec Alpha 300), allowing spectra acquisition in both upright and inverted microscope configuration. The Raman probe was a frequency doubled Nd-YAG laser ($\lambda = 532$ nm), focused on the sample through a 60X dry objective. Back-scattered photons were collected through the same focusing objective, and, after passing through an edge filter, sent to the spectrometer via a 50- μm core fiber. Spectra were acquired in the 300-4000 cm^{-1} range by using a 600 g mm^{-1} grating. Spontaneous and SERS Raman spectra were acquired by using laser powers of ~ 0.5 mW and ~ 10 μW , respectively.

2.2 Samples preparation

SERS substrates characterizations in terms of EF was performed by using Crystal Violet (CV) as probe molecule. At this purpose, a sandwiched cell was created by glowing a SERS substrate and a glass coverslip by using two parafilm strips. Then, a proper aliquot of 1 μM CV solution was infiltrated in the cell and allowed to dry at room temperature. The use of such methodology improves the uniformity of molecule distribution on the SERS substrate, strongly reducing the well-known coffee-ring effect. Moreover, by accurately measuring the cell volume, a more reliable estimation of the number of molecules infiltrated in the cell can be obtained. In this condition, assuming an even distribution of molecules on the two sandwiched cell walls, the molecular density of CV molecules on the SERS substrate can be estimated to be around $3.9 \cdot 10^4$ $\text{mol}/\mu\text{m}^2$.

3. RESULTS AND DISCUSSION

3.1 SERS substrates fabrication

SERS substrates were prepared following a procedure similar to that reported in ref. [9], where Ag-based coral-like nanotextures were created on oxidized Silicon based AFM-tips in order to enhance their plasmonic activity for TERS (Tip-Enhanced Raman Spectroscopy) applications. In the present case, the Ag-texture was created on commercial glass coverslips, as described below.

In the first step, glass coverslips were pre-cleaned in a RF discharge, in order to remove the presence of contaminants that could affect the successive metal deposition. At this purpose, the coverslips were exposed to an Argon-based plasma, obtained by using an ICP plasma system (Harrick Plasma, PDC-32G-2). In this phase, the Ar pressure in the RF chamber was 1 Torr and the RF power was set to 18W. Therefore, an adhesion bilayer, consisting of a 3 nm Cr layer and an overlying 10 nm Au layer, was sputtered on the coverslip. Sputtering was performed by using a magnetron sputtering system (Quorum, Q300TD). This latter is endowed with two independent sputtering heads, therefore allowing the sequential sputtering of two metals without breaking the vacuum in the chamber, and two quartz microbalances, for an optimal control of the film thickness during the sputtering process. The sputtering currents for Cr- and Au-layer deposition were $I_{\text{Cr}}=120$ mA and $I_{\text{Au}}=20$ mA, respectively. After that, a 30 nm thick Ag-layer was deposited on the bilayer, by using a sputtering current $I_{\text{Ag}}=50$ mA. Fig. 1, part a, report a Scanning Electron Microscope (SEM) image of the so obtained substrate. As it is possible to note, it appears quite smooth on nanometric scale, so that its plasmonic activity can be expected to be quite low. In order to improve the substrate roughness, it was exposed for 90 s to an ICP treatment, by using the same system used to clean the substrate but using as feeding gas synthetic air (79% N_2 + 21% O_2 mixture). This treatment strongly

increases the Ag layer roughness. As side effect, exposure to atomic oxygen produced in the in the discharge leads to the formation of a thin Ag-oxide layer. Very likely, this oxide layer contributes, with SSD, to the formation of the nanoporous structures that we observe. At the same time, however, the presence of the oxide limits the SERS response and therefore it has to be removed. Therefore, in order to restore the pristine metallic character of the Ag layer, a further plasma treatment, but in Argon atmosphere ($p=0.6$ Torr), was applied to reduce the oxide [10]. This reduction is obtained by the electrons of the plasma and by UV photons, which contribute to break the silver–oxygen bond. The effectiveness of this reduction process was confirmed by X-rays diffraction (XRD) analysis, as shown in the following.

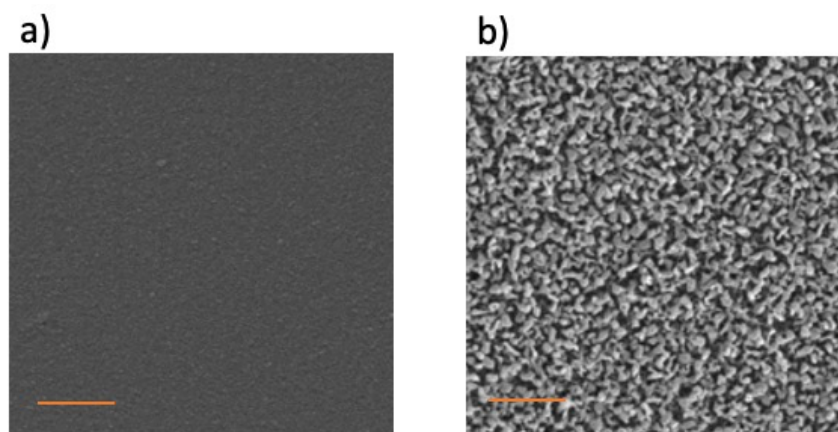


Figure 1. Comparison between the Ag layer morphology before (part a) and after (part b) the complete ICP treatment (air- and Ar-based plasma), obtained by SEM analysis (scale bar = 1 μm).

3.2 SERS substrates characterization

Previous to plasmonic evaluation, the so obtained substrates were first characterized from a morphological point of view. At this purpose, SEM images were processed in order to get a binarized image suitable to calculate the FFT first and the Power Spectral Density (PSD) afterwards, according to the relation:

$$PSD(v_x, v_y) = \frac{1}{N_x^2 N_y^2} \frac{|U(v_x, v_y)|^2}{\Delta v_x \Delta v_y} \quad (1)$$

where $U(v_x, v_y)$ is the 2D FFT of the image, N_x and N_y the total number of points in each domain and Δv_x and Δv_y the data point spacing in the frequency space. Finally, rotational average of PSD function (r-PSD) was calculated. A typical result is shown in Fig. 2, part a. Clearly, the existence of a peak in the PSD indicates the existence characteristic length λ_c in the Ag nanostructures pattern, which is related to the peak frequency v_c by the relation $\lambda_c=1/v_c$. The degree of “order” found could be a signature of a mechanism ascribable to SSD [11,12]. In fact, a thin metal film is intrinsically unstable and tends to dewet even at temperatures well below the melting points of their bulk counterparts. The film is destabilized when energy is supplied to atoms of the metallic film, so that intermolecular forces can overcome the stabilizing effect of interfacial tension. Therefore, film rupture can take place and the film evolves to more complex morphologies. Intriguingly, this newly developed morphologies present a characteristic length, that can be tuned by changing the film thickness [12]. For a film 30 nm thick and exposed to the air-RF plasma for 90 s, r-PSD exhibits a peak at $v_c=3.8 \cdot 10^{-3} \text{ nm}^{-1}$, so that $\lambda_c=263$ nm.

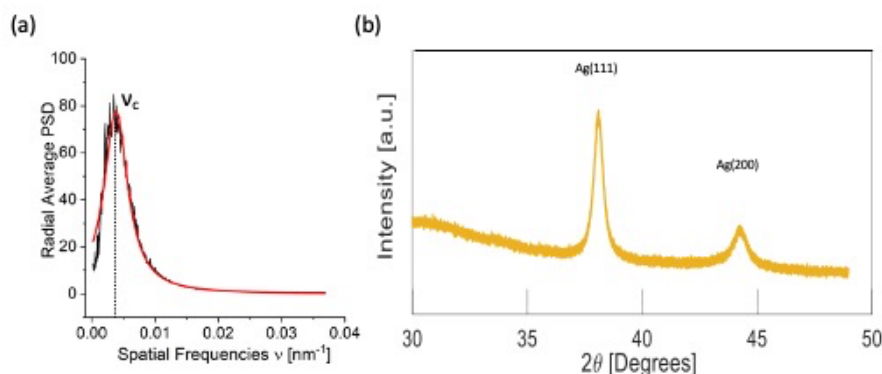


Figure 2. a) Radial average of the PSD function obtained by analyzing the SEM image reported in Fig 1a. The presence of a peak in the PSD testifies the presence of an intrinsic “ordering” mechanism ruling the formation of the observed Ag nanostructures. b) XRD analysis of the Ag layer, following the complete ICP treatment. The labels correspond to the assignment of the observed XRD features.

As a further step, we characterized the SERS substrate by X-ray diffraction (XRD). A typical XRD spectrum is shown in Fig. 2, part b. It exhibits two peaks at at 38.2° and 44.3°, corresponding to signals from the (1 1 1) and (2 0 0) planes of the face centered Ag cubic structure. These features give evidence of the polycrystalline phase associated to the Ag film. Moreover, the absence of features associated to Ag_xO species in the 30°-34° 2θ pattern is indicative of a complete reduction of Ag_xO species to metallic Ag.

Finally, SERS response of our substrates was characterized in terms of the EF using CV as probe molecule. In particular, starting from a 1 μ M CV solution, a uniform distribution of molecules adhered on the SERS substrate was prepared, according to the procedure described in the Materials and Methods paragraph. Therefore, SERS signals were acquired by raster scanning in a 10x10 μ m² region and the average signal was calculated (see Fig.3). It is worth noticing that SERS features are also present in the region around 3000 cm⁻¹, which suggests a broad plasmonic response of the SERS substrate. For comparison, the spontaneous Raman signal corresponding to a 5.57 mM CV concentration was also acquired.

The EF was therefore obtained, according to the relation [5]:

$$EF = \frac{N_R I_S P_R \tau_R}{N_S I_R P_S \tau_S} \quad (2)$$

As usual, SERS and spontaneous Raman signals, I_S and I_R , were normalized to the respective number of molecules (N_S and N_R), laser powers (P_S and P_R) and integration time (τ_S and τ_R). The intensities of SERS and spontaneous Raman signals were evaluated at ~ 1580 cm⁻¹. The number of molecules N_S adsorbed on the SERS substrate in the confocal laser spot area $A_C = 0.44$ μ m² was $\sim 1.72 \cdot 10^4$ while the number of molecules N_R contained in the confocal detection volume $V_C = 2.3$ fL was $N_R \sim 7.7 \cdot 10^6$. According to these values, Eq. 2 finally provides $EF \sim 1.1 \cdot 10^7$. Similar values were found obtained by other raster scanning measurements in different regions of the substrate. These outcomes clearly suggest interesting enhancements and a reasonable reproducibility of our substrates which combined to a quite easy and relatively cheap fabrication route render our approach very promising for further improvements. Indeed, some crucial parameters, such as the film thickness and the exposure time to the air-RF plasma, need a systematic study to optimize our protocol. Moreover, the spatial uniformity has also to be fully evaluated, together with the spectral response in the entire VIS-IR region.

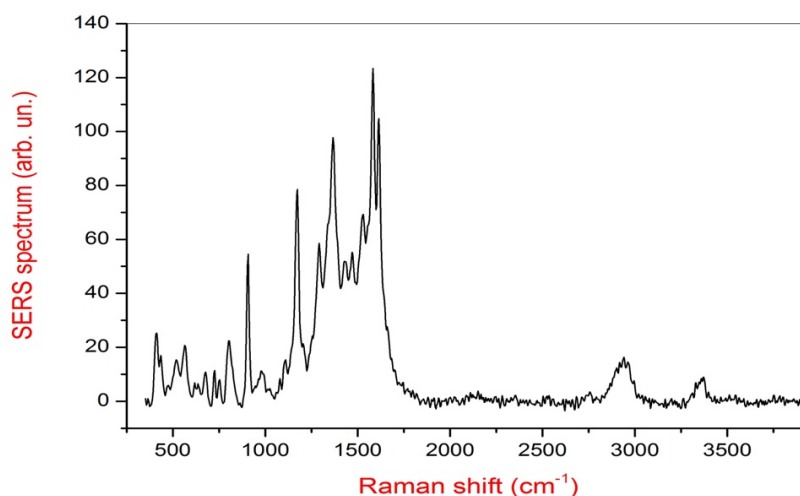


Figure 3. SERS signal corresponding to a 1 μM CV concentration. It was obtained by averaging SERS signals acquired in a $10 \times 10 \mu\text{m}^2$ region.

REFERENCES

- [1] M. Sui, S. Kunwar, P. Pandey, J. Lee “Strongly confined localized surface plasmon resonance (LSPR) bands of Pt, AgPt, AgAuPt nanoparticles” *Sci. Rep.* 9, 16582 (2019).
- [2] V. Amendola, O.M. Bakr, F. Stellacci “A Study of the Surface Plasmon Resonance of Silver Nanoparticles by the Discrete Dipole Approximation Method: Effect of Shape, Size, Structure, and Assembly” *Plasmonics* 5, 85–97(2010).
- [3] G. Rusciano, P. Capriglione, G. Pesce, S. Del Prete, G. Cennamo, D. Di Cave, L. Cerulli, A. Sasso “Raman Microspectroscopy Analysis in the Treatment of Acanthamoeba Keratitis” *PLoS One.* 8(8): e72127 (2013).
- [4] K. Kong, C.J. Rowlands, S. Varma, W. Perkins, I.H. Leach, A.A. Koloydenko, H.C. Williams, I. Nottingher “Diagnosis of tumors during tissue-conserving surgery with integrated autofluorescence and Raman scattering microscopy” *PNAS* 110(38), 15189-15194 (2013).
- [5] X. Lin, Y. Cui, Y. Xu, B. Ren, Z. Tian “Surface-enhanced Raman spectroscopy: substrate-related issues” *Anal. Bioanal. Chem.* 394, 1729-1745 (2009).
- [6] E. C. Le Ru, P. G. Etchegoin, “Single-molecule surface-enhanced Raman spectroscopy” *Ann. Rev. Phys. Chem.* 63, 65-87 (2012).
- [7] K. Kneipp, Y. Wang, H. Kneipp, L.T. Perelman, I. Itzkan, R.R. Dasari, M.S. Feld “Single Molecule Detection Using Surface-Enhanced Raman Scattering (SERS)” *Phys. Rev. Lett.* 78, 1667 (1997).
- [8] G. Zito, G. Rusciano, G. Pesce, A. Dochshanov, A. Sasso “Surface-enhanced Raman imaging of cell membrane by a highly homogeneous and isotropic silver nanostructure” *Nanoscale*, 7, 8593-8606 (2015).
- [9] A. Capaccio, A. Sasso, O. Tarallo, G. Rusciano “Coral-like plasmonic probes for tip-enhanced Raman spectroscopy” *Nanoscale*, 12, 24376-2438(2020).
- [10] V. Ovchinnikov, ICQNM 2016: The Tenth International Conference on Quantum, Nano/Bio, and Micro Technologies 6–11 (2016).
- [11] P. de Gennes, F. Brochard-Wyart and D. Quere, *Capillarity and Wetting Phenomena*, 6th ed, Springer, New York, NY, (2004).
- [12] C.V. Thompson “Solid-State Dewetting of Thin Films” *Annu. Rev. Mater. Res.* 42, 399–434 (2012).